Pressure-Induced Symmetry-Lowering Transition in Dense Nitrogen to Layered Polymeric Nitrogen (LP-N) with Colossal Raman Intensity

Dane Tomasino, Minseob Kim, Jesse Smith, and Choong-Shik Yoo

Phys. Rev. Lett. **113**, 205502 — Published 12 November 2014

DOI: 10.1103/PhysRevLett.113.205502

Pressure-induced Symmetry Lowering Transition in Dense Nitrogen to Layered Polymeric Nitrogen (LP-N) with Colossal Raman Intensity

Dane Tomasino,[1] Minseob Kim,[1] Jesse Smith,[2] and Choong-Shik Yoo[1*]

1 *Department of Chemistry and Institute for Shock Physics, Washington State University, WA 99164*

2 *High Pressure Collaborating Access Team at Advanced Photon Source, Geophysical Laboratory, Carnegie Institution of Washington, Argonne, Illinois 60439*

* *Correspondence to csyoo@wsu.edu; (509) 335 - 2712*

Abstract

We present the discovery of novel nitrogen phase synthesized using laser-heated diamond anvil cells at pressures between 120-180 GPa well above the stability field of *cubic gauche(cg)*-N. This new phase is characterized by its singly bonded, layered polymeric (LP) structure similar to the predicted *Pba2* and two colossal Raman bands (at ~1000 and 1300 cm^{-1} at 150 GPa), arising from two groups of highly polarized nitrogen atoms in the bulk and surface of the layer, respectively. The present result also provides a new constraint for the nitrogen phase diagram, highlighting an unusual symmetry lowering *3D cg*- to *2D* LP-N transition and thereby the enhanced electrostatic contribution to the stabilization of this densely packed LP-N (ρ = 4.85 g/cm^3 at 120 GPa).

The ability to modify chemical bonding and crystal structure of solids by means of high-pressure and high-temperature opens new opportunities to development of novel materials with unique properties. Recent high-pressure experiments and theoretical calculations have shown that highly compressed molecular solids transform into extended solids with more itinerant electrons in covalent or metallic network structures [**1-5**]. These molecular-to-nonmolecular transitions occur as a result of electron delocalization arising from a rapid increase in electron kinetic energy at high density. As such, they often lead to densely packed, "fully saturated" or wide bandgap polymeric covalent solids in extended three-dimensional (*3D*) networks of corner (or edge)-sharing polyhedral. The pressure-induced broadening of the electronic bands, on the other hand, may lead to an insulator–metal transition, providing a competing mechanism.

Upon further compression, valence electrons of the extended solids can even ionize to form amorphous or ionic solids, as the electrostatic forces become dominant. This pressure-induced ionization will ultimately lead to chemical disassociation to elemental solids or atomistic metals, which can be related to those entropy-driven conducting fluids at high temperatures. Importantly, at a given density a delicate balance between electron delocalization (governing bonding) and ionization (governing packing) can give rise to subtle structural symmetry-breaking distortions, resulting in complex structures [**1,2**] and novel properties such as superhardness, superconductivity and nonlinear optical properties [**3-5**].

Nitrogen is the first molecular system predicted to transform into a polymeric form prior to the metallization [**6**], which has been discovered later in laser-heated diamond anvil cell (DAC) experiments above 110 GPa and 2000 K [**7,8**]. This successful

prediction of *cg*-N [**6**] has stimulated the search for other singly bonded polymeric forms of nitrogen and other molecular solids. As result, a large number (over dozen) of extended nitrogen structures have been predicted to be stable, both in the stability field of *cg*-N such as α-arsenic, chain, layered, ring structures, and a metastable form of *cg*-N (*C2/c*) [**9-13**], and above the stability field such as the layered *Pba2* or *Iba2* structures (188–320 GPa), the helical tunnel $P2_12_12_1$ structure (>320 GPa), and the cluster form of nitrogen diamondoid (>350 GPa) [**14-17**].

Despite extensive theoretical and experimental efforts, the synthesis of the predicted phases has been challenging. To this date, the *cg*-N is still the only extended phase of nitrogen discovered. Therefore, it is timely and also important to demonstrate the existence of theoretically predicted structures in dense nitrogen. This is exactly what we report in this Letter; that is, the discovery of a new extended nitrogen phase in the proposed layer *Pba2* structure, formed above the stability field of *cg*-N. Interestingly, this new, layered polymeric nitrogen (LP-N) exhibits novel properties such as the colossal Raman cross section – probably the largest of all solids, and provides new constraints on the nitrogen phase diagram underscoring an unusual, symmetry-lowering transition from *3D* cg-N to *2D* LP-N transition in dense nitrogen.

All samples were prepared using a He-gas driven membrane DAC with 0.1 mm culet diamonds. Rhenium was used as gasket material pre-compressed to 0.025 mm thickness with a sample chamber drilled using electric discharge machining to produce a 50 μm diameter hole. Nitrogen gas of 99% purity was loaded at around 2000 atmospheres using an in-house gas loading device. The nitrogen sample pressure was monitored through the use of the calibrated ν_1 vibrational frequency [**18**] and the high frequency

edge of the diamond phonon [**19**]. Raman spectra of the nitrogen samples were collected with a custom built confocal micro-Raman optical assembly with a 532 nm excitation laser and an Andor iXon CCD detector. Samples were laser heated using 1070 nm IPG Photonics ytterbium fiber laser. X-ray diffraction experiments were conducted at the HPCAT beamline (16IDB) at the Advanced Photon Source of Argonne National Laboratory. Highly focused (~ 0.01 mm diameter) monochromatic x-rays (λ = 0.406 Å) were used to produce angle dispersive x-ray diffraction images collected with a high-resolution area detector (marCCD). Special care was exercised to place the cleanup slit close to the sample (within 2-3 cm) and obtain the gasket free diffraction pattern.

The nitrogen samples were compressed to pressure greater than 100 GPa where they can absorb laser radiation and be heated directly without the addition of a thermal absorber. Samples were heated to temperatures as high as 3000 K as evidenced by the bright glowing of the thermal radiation and measurement through optical pyrometry [**20**]. Temperatures were difficult to measure precisely as the laser-sample coupling is unstable, creating temperature fluctuations, and temperature gradients beyond the laser spot are quite large. Thus temperature measurements are unreliable in terms of accuracy but provide valuable insight into the approximate magnitude of the highest temperatures reached during heating experiments. The sample is laser heated from one side, that axial thermal gradients are irrelevant considering the larger radial thermal gradient and, above all, the huge thermal fluctuations due to the instable laser-sample coupling. This unstable coupling prevented in situ high pressure-high temperature diffraction.

Laser heating samples at pressures greater than 125 GPa typically resulted in the molecular to non-molecular chemical reaction as nitrogen is transformed into the black

amorphous phase or *cg*-N phase [**7,8**] if heated above 2000 K. This is evident by the formation of clear spots in the otherwise dark molecular nitrogen phase. The formation of *cg*-N has been well documented; however, within some of the clear spots the nitrogen showed immensely intense low-frequency Raman features that are uncharacteristic to any known nitrogen phase (depicted as LP-N in **Fig. 1**). This is seen in the inset: Spot A is the black amorphous phase with no sharp Raman feature, Spot B is the newly formed, transparent LP-N phase with two strong Raman peaks at ~1005 and 1300 cm^{-1}, and Spot C is the previously known *cg*-N phase with the characteristic phonon at 875 cm^{-1} at 150 GPa. The pressure-dependent spectral changes of LP-N phonons (**Fig. S1**) suggest a fairly stiff lattice and shift nearly linearly with pressure at approximately 1.6 and 1.2 cm^{-1}/GPa, respectively, above 90 GPa. Below this pressure, the low-frequency phonon shifts somewhat faster at ~2.5 cm^{-1}/GPa. Note that there are several very weak Raman features observed at around 900 cm^{-1} and 1100 cm^{-1} at 150 GPa in Fig. 1, which might come from LP-N, cg-N, or even other nitrogen phases (see **Fig. S1**). The Raman cross section of LP-N is estimated to be $1.2 * 10^{-28}$ cm^2/sr, approximately three times that of diamond single crystal and possibly the largest of all solids (**Fig. S2**).

The LP-N phase has been produced in four separate experiments at 126, 150, 156, and 175 GPa, at ambient temperature. In every case a mixture of amorphous, LP-N, and *cg*-N phase was produced. Heating below 126 GPa typically results in *cg*-N without the presence of new LP-N. The substantially higher synthetic pressure than that of cg-N at 110 GPa [7,8] is likely the reason why this new extended phase of nitrogen was not observed previously. Efforts to recover these extended phases to pressures below 50 GPa were unsuccessful due to catastrophic diamond failure. No apparent evidence was found

in the visual, spectral and diffraction data, indicating chemical reaction of nitrogen with diamond and gasket.

X-ray diffraction patterns were obtained from the center of laser heating spot after heating while unloading pressure from 137 GPa to 52 GPa (**Fig. 2**), showing highly preferred orientations (**Fig. S3**). Nevertheless, the majority of diffraction peaks observed can be indexed in terms of the theoretically suggested *Pba2* structure (**Fig. 3**), with a few exceptions of weak features at $2\theta \sim 8^{o}$ and 10^{o}. These minor features can be interpreted in terms of the C2/c structure, also predicted to be a metastable form of *cg*-N [**13**]. A small poorly resolved feature at $2\theta \sim 7^{o}$ is likely from the diffraction pattern from unreacted θ-N_2 [**21**]. On the other hand, the presence of *cg*-N cannot be ruled out, as its diffraction lines overlap with those of the cubic-like *Pba2*.

A full-pattern Rietveld refinement of the present diffraction pattern is, however, challenging because of the highly preferred orientation. Therefore, we have used a Le Bail method to determine the structural parameters such as the background, zero shift, peak profiles, and lattice parameters, using the theoretically predicted atomic parameters [**14**]. While the fitted result (**Fig. 3**) is reasonably good, note that the calculated intensity profile for the *Pba2* has nearly no diffraction intensities along the [002] direction including those of (002), (201), (021), and so on. In fact, this is consistent with the systematic absence of (00*l*) in the *Pba2* space group [**22**]. Furthermore, in a non-hydrostatic condition the basal plane of a layered structure (i.e., (002) in the *Pba2*) often stacks up normal to the primary stress direction along the incoming x-rays, causing a substantially reduced diffraction intensity of this plane with respect to those perpendicular to (i.e., (200) and (020) in the *Pba2*) [**23**].

Within the three-phase model, the best fit results in the lattice parameters at 112 GPa: a=4.1602 Å, b=4.2481 Å, c=4.3689 Å, and density ρ = 4.820 g/cm^3 for LP-N in the *Pba2*, a=3.4694 Å, ρ = 4.456 g/cm^3 for *cg*-N in the $I2_13$, and a=4.9458 Å, b=3.5586 Å, c=4.6738 Å, and β=90.10^o with ρ = 4.524 g/cm^3 for the *C2/c*. These structures result in a similar single bond N-N distance of ~1.35 (±0.01) Å for all three structures, and the pressure-volume compression curves for both LP-N and *cg*-N (**Fig. 4**). Clearly, the present results are in excellent agreements with the previously measured and calculated values in Refs. [**7,8,14**], as well as with the third-order Birch-Murnaghan EOS fits (solid and dotted lines) (see also **Fig. S4**). Note that LP-N (ρ= 4.85 g/cm^3) is ~7.8% denser than *cg*-N (4.50 g/cm^3) at 120 GPa and also ~22.5% stiffer: $B_o(B')$ =342 (6.0) GPa vs. 279 (4.8) GPa.

The present structural model explains the presence of two major ν_s(N-N) vibrations in LP-N (**Fig. 1**). In the *Pba2* structure, nitrogen atoms are distributed among four equally weighted sites forming *2D* layers of fused seven membered nitrogen rings along the [001] direction. Each layer is made of two equivalent N1(0.293, 0.217, 0.661) and N2(0.785, 0.217, 0.340) sites in the bulk, where nitrogen atoms form a nearly ideal (<NNN=120(±5)^o, $\underline{sp^2}$-hybridized) three-fold coordination, and two other N3(0.021, 0.336, 0.177) and N4(0.838, 0.017, 0.822) sites on the surface, where nitrogen atoms form a buckled (<NNN=100(±10)^o, sp^3-hybridized) three-fold coordination, analogous to that in *cg*-N. The only difference in the latter is that the N-N bonds are eclipsed in LP-N, but staggered in *cg*-N. A consequence of this lattice polarization is the splitting of lattice phonon into two: the $\nu_s^+(sp^2)$ at 1300 cm^{-1} representing the vibration of the bulk nitrogen atoms in N1 and N2 sites and the $\nu_s^-(sp^3)$ at 1000 cm^{-1} of the surface nitrogen at the N3

and N4 sites, as observed at 150 GPa. Then, the 100 cm^{-1} difference between the ν_s^- of LP-N and the ν_s of *cg*-N can be understood in terms of the 7.8% density difference with a typical mode Grüneisen parameter γ~1.3 for covalent solids in $\gamma = - \delta \ln\nu / \delta \ln V$ [**24**].

The present discovery of LP-N provides new constraints for the phase diagram of nitrogen (**Fig. 4 inset**). At low pressures, nitrogen represents a classical diatomic molecular system with a strong triple bond (N≡N), exhibiting fascinating polymorphism with four solid molecular phases (α, β, γ, δ) below 10 GPa and 300 K [**25,26**]. Upon further compression, δ-N_2 undergoes a series of structural transitions to ε-, ζ- and amorphous black η-N_2 at ambient temperature and to ε-, θ- and □morphous "□□□"–N_2 at high temperatures [**8,21,27**]. These transitions are, however, known to show strong path dependencies, underscoring the intermediary nature of bonding in these phases between molecular (below 60-80 GPa) and extended solids (above 100-120 GPa). Above 120 GPa, nitrogen becomes fully extended to form *cg*-N and LP-N. The phase boundaries are difficult to determine, as these transitions are often controlled kinetically (signified by the dashed lines). Nevertheless, we suggest a positive slope for the *cg*- and LP- phase boundary, based on (i) the higher density of LP-N compared to *cg*-N, (ii) the strong presence of *cg*-N in the stability field of LP-N (not the other way), and (iii) the absence of LP-N in the stability field of *cg*-N between 100 and 125 GPa. The melting line of *cg*-N and the liquid-liquid transition line (dotted lines) are reproduced from those predicted theoretically [**28,29**].

The above-described phase diagram underscores the pressure-induced *3D-to-2D* structural transition, in contrast to more commonly observed *2D*-to-*3D* transitions at high pressures as in, for example, the graphite-to-diamond transition. However, several recent

theoretical calculations have predicted the stabilization of *2D* layer structures at very high presssures. Those predictions include *2D* polymeric-CO in *Cmcm* [**30**], partially ionized extended layers of H_2O in $P2_1$ [**31**], and the graphene-like structure suggested for recently discovered H_2-IV [**32,33**]. In this regard, the *cg*- to LP-N transition is not surprising, but have significant implications to those transitions in other molecular systems and, together, begin to provide new fundamental insights into the pressure-induced ionization overtaking the pressure induced hybridization in densely packed molecular systems.

Finally, the newly discovered LP-N exhibits novel properties including its colossal Raman cross section – presumably the largest of all solids, high density (ρ_o = 4.0 g/cm^3) even compared to diamond, 3.5 g/cm^3, high stiffness (B_o=345 GPa) rivaling superhard *cubic*-BN, and potentially high energy density as predicted for *cg*-N. Therefore, LP-N constitutes a class of novel materials joining diamond and *cubic*-BN. Demonstrated the existence of LP-N and its interesting layer structure and novel properties, the present result will certainly stimulate new research efforts to develop and/or search for similar densely packed layer structures– not necessarily at high pressures but even at ambient conditions through alternate synthetic routes.

We thank Dr. Christian Mailhiot for stimulated scientific discussion. The present study has been supported by NSF-DMR (Grant No. 1203834) and DTRA (HDTRA1-12-01-0020), and DCO-EPC. The x-ray work was performed at the HPCAT in support of CDAC. HPCAT operations are supported by DOE-NNSA (DE-NA0001974) and DOE-BES (DE-FG02-99ER45775).

References

1. M. Hanfland, K. Syassen, N.E. Christensen, et al., *Nature* **408**, 174 (2000).

2. Y. Ma, M.I. Eremets, A.R. Oganov, et al., *Nature* **458**, 182 (2009).

3. J. Lipp, W.J. Evans, B.J. Baer, et al., *Nature Mat.* **4**, 211 (2005).

4. V. Iota, C. S. Yoo, H. Cynn, *Science* **283**, 1510 (1999).

5. R.P. Dias, C. S. Yoo, V.V. Struzhkin et al., *Proc. Nat. Acad. Sci.* **110,** 11720 (2013).

6. C. Mailhiot, L. H. Yang, A. K. McMahan, *Phys. Rev. B* **46**, 14419 (1992).

7. M. I. Eremets, A. G. Gavriliuk, I. A. Trojan, et al., *Nature Materials* **3**, 558 (2004).

8. M. J. Lipp, J.-H. Klepeis, B. Baer, et al., *Phys. Rev. B.* **76**, 014113 (2007).

9. R.M. Martin and R.J. Needs, *Phys. Rev. B* **34**, 5082 (1986).

10. S.P. Lewis and M.L. Cohen, *Phys. Rev. B* **46**, 11117 (1992).

11. W.D. Mattson, D. Sanchez-Portal, et al., *Phys. Rev. Lett.* **93**, 125501 (2004).

12. F. Zahariev, A. Hu, J. Hooper, et al., *Phys. Rev. B* **72**, 214108 (2005).

13. Y. Yao, J.S. Tse, K. Tanaka, *Phys. Rev. B* **77**, 052103 (2008).

14. Y. Ma, A.R. Oganov, Z. Li, et al., *Phys. Rev. Lett***. 102**, 065501 (2009).

15. J. Sun, M. Martinez-Canales, D.D. Klug, et al., *Phys. Rev. Lett*. **111**, 175502 (2013).

16. J. Kotakoski and K. Albe, *Phys. Rev. B* **77**, 144109 (2008).

17. X. Wang, Y. Wang, M. Miao, et al., *Phys. Rev. Lett*. **109**, 175502 (2012).

18. H. Olijnyk and A.P. Jephcoat, *Phys. Rev. Lett***. 83**, 332 (1999)

19. Y. Akahama, H. Kawamura, *J. Appl. Phys***. 100**, 43516 (2006).

20. D. Tomasino, Z. Jenei, W. Evans, and C.S. Yoo, *J. Chem. Phys*. **140**, 244510 (2014).

21. E. Gregoryanz, A.F. Goncharov, R.J. Hemley et al., *Phys. Rev. B* **66**, 224108 (2002).

22. See, *International Tables for Crystallography*, vol A, p48, the 5th edition by T. Hahn (Springer, 2005).

23. S. Merkel and T. Yagi, *J. Phys. Chem. Solids* **67**, 2119 (2006).

24. T. Soma and K. Kudo, *J. Phy. Soc., Jpn*. **48**, 115 (1980).

25. D. Schiferl, S. Buchsbaum, and R.J. Mills, *J. Phys. Chem*. **89**, 2324 (1985).

26. R. Bini, L. Ulivi, J. Kreutz, and H.J. Jodl, *J. Chem. Phys***. 112**, 8522 (2000).

27. A.F. Goncharov, J.C. Crowhurst, V.V. Struzhkin et al., *Phys. Rev. Lett.* **101**, 95502 (2008).

28. B. Boates and S. A. Bonev, *Phys. Rev. Lett***. 102**, 015701 (2009).

29. D. Donadio, L. Spanu, I. Duchemin, et al., *Phys. Rev. B* **82**, 020102(R) (2012).

30. J. Sun, D.D. Klug, C.J. Pickard, et al., *Phys. Rev. Lett.* **106**, 145502 (2011).

31. A. Hermann, N.W. Ashcroft, R. Hoffmann, *Proc. Nat. Acad. Sci.* **109,** 745 (2012).

32. R.E. Cohen, I.I. Naumov, R.J. Hemley, *Proc. Nat. Acad. Sci.* DOI: 10.1073/pnas.1312256110 (2013).

33. V. Labet, P. Gonzalez-Morelos, R. Hoffmann, et al., *J. Chem. Phys.* **136**, 076501 (2012) and *ibid* 136, 074502 (2012).

34. E. Knittle, R. M. Wentzcovitch, R. Jeanloz, et al., *Nature* **337**, 349 (1989).

Figure Captions

Fig. 1 (Left) Raman spectra of laser-heated nitrogen at 150 GPa and ambient temperature, obtained in three distinctive regions in the inset: (A) black amorphous, (B) new LP-N, and (C) *cg*-N. Note that LP-N shows two characteristic peaks with exceptionally strong intensities. (Right) The pressure dependent shifts of two characteristic ν_s(N-N) of LP-N shown in comparison with that of *cg*-N. The red circles are reproduced from Refs. **7** and 8.

Fig. 2 Angle-resolved x-ray diffraction patterns obtained from laser-heated nitrogen in the pressure range between 137 and 52 GPa as pressure decreases, plotted after subtracting the background (see Fig. **S3**).

Fig. 3 (Top) The angle-resolved x-ray diffraction pattern of laser-heated nitrogen at 112 GPa, showing together with the three-phase refined and difference patterns. The refined results of individual phases are also plotted below for the major LP-N phase in *Pba2* in black and two minor phases, *cg*-N (*$I2_13$*) in red and its metastable form in C2/c in orange. The hkl's of each phases are labeled, and their positions marked as the vertical bars. (Bottom) Crystal structures of the proposed phases showing the layered *Pba2* structure made of seven-membered N-N (N_7) rings in comparison with the *$I2_13$* and *C2/c* structures made of even number N_{10} and N_{12} rings in *3D* networks, respectively.

Fig. 4 The pressure-volume compression curves and third-order Birch-Murnaghan EOS fits of LP-N (circles and solid line) and cg-N (squares and dotted line), plotted in comparison with the previous data (triangles in [7] and diamonds in [8]) and the calculated *Pba2* structure (cross in [14]). (Inset) The proposed phase diagram to

emphasize the presence of new extended LP-N above the stability field of *cg*-N. The dotted lines are from the previous calculations [28,29] and the dashed lines signify the kinetic lines.

Fig. 1

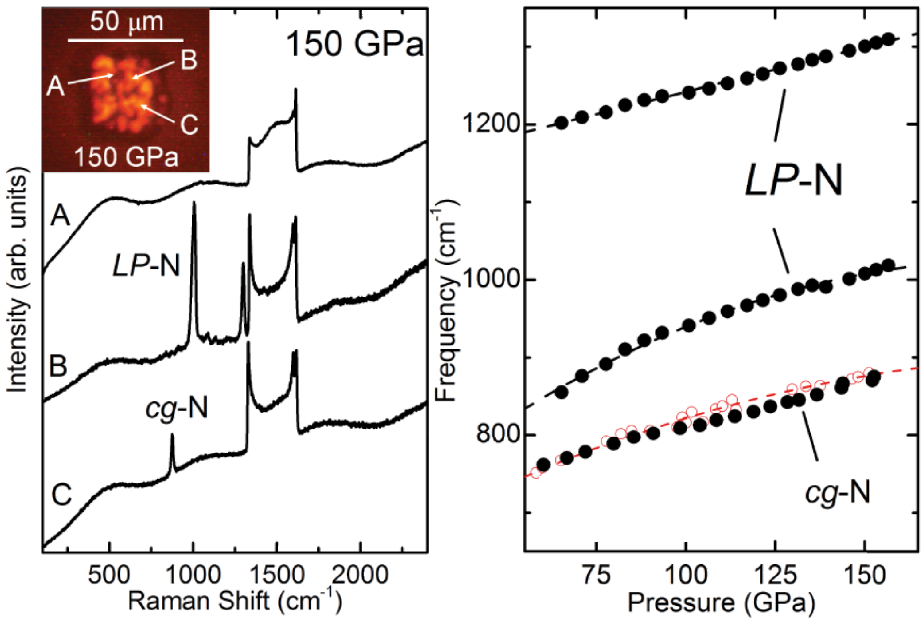

Figure 1 LS14571 15OCT2014

Fig. 2

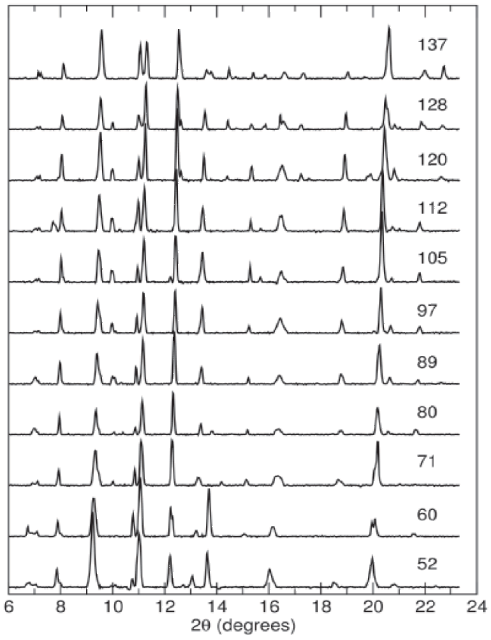

Figure 2 LS14571 15OCT2014

Fig. 3

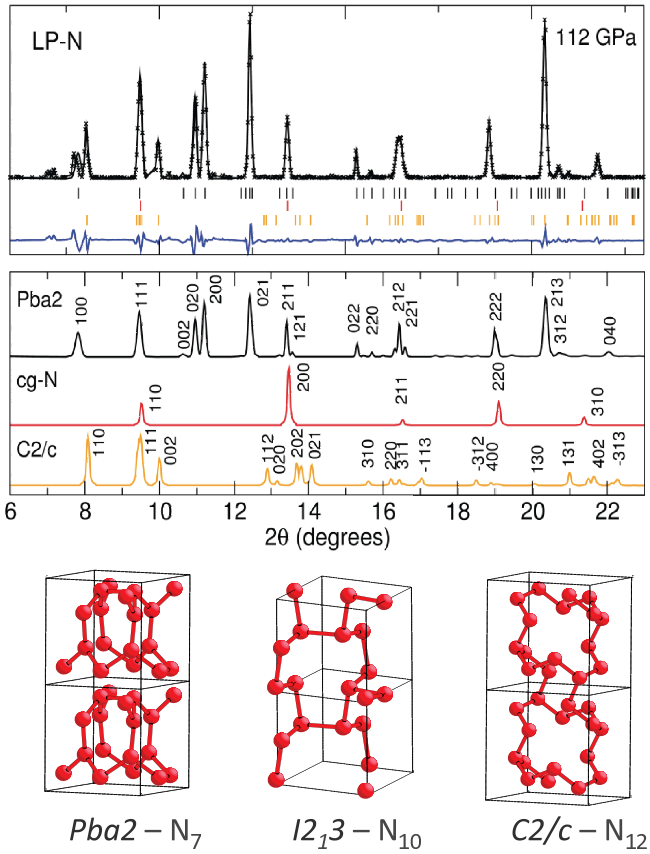

Figure 3 LS14571 15OCT2014

Fig. 4

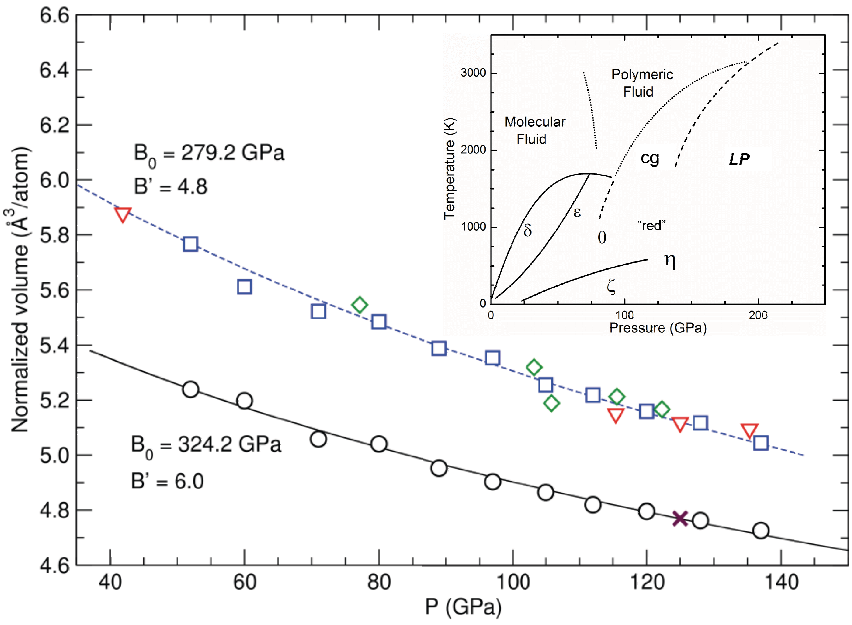

Figure 4 LS14571 15OCT2014